Electronic Supplementary Information (ESI)

On the Impact of Selective Donor:Acceptor Structural Ordering in PBDB-T:ITIC Organic Solar Cells

Xabier Rodríguez-Martínez[1]*, *Sara Marina*[2], *Albert Harillo-Baños*[3], *Mariano Campoy-Quiles*[3], *Jaime Martin*[1,2]*

[1] Centro de Investigación en Tecnoloxías Navais e Industriais (CITENI), Universidade da Coruña, Ferrol, 15403, Spain
[2] POLYMAT, Universidad del País Vasco, Donostia-San Sebastián, 20018, Spain
[3] Instituto de Ciencia de Materiales de Barcelona (ICMAB-CSIC), Bellaterra, 08193, Spain

* Corresponding authors: xabier.rodriguez@udc.es, jaime.martin.perez@udc.es

Experimental Section

Materials and solvents: PBDB-T (poly[(2,6-(4,8-bis(5-(2-ethylhexyl)thiophen-2-yl)-benzo[1,2-*b*:4,5-*b*']dithiophene))-*alt*-(5,5-(1',3'-di-2-thienyl-5',7'-bis(2-ethylhexyl)benzo[1',2'-*c*:4',5'-*c*']dithiophene-4,8-dione)]) with a M_w of 70.5 kg mol^{-1} and ITIC (3,9-bis(2-methylene-(3-(1,1-dicyanomethylene)-indanone))-5,5,11,11-tetrakis(4-hexylphenyl)-dithieno[2,3-d:2',3'-d']-s-indaceno[1,2-b:5,6-b']dithiophene) were obtained from Ossila Ltd. As solvents, chlorobenzene (CB), chloroform (CF), ortho-xylene (o-xy), and 1,8-diiodoctane (DIO) were purchased from Merck and used as received. To clean the substrates, analytic grade acetone, 2-propanol, sodium hydroxide 10 vol% and Hellmanex solution diluted at 10% in water were acquired from Merck and Labbox and used as received.

Film preparation: The polymer and small molecule films used for GIWAXS experiments were deposited by spin-coating (2000 rpm, 60 s) from 20 mg·mL^{-1} solutions. Prior to depositions, the solutions were stirred during minimum 2 hours to overnight at 35 ºC for samples dissolved in CF and 80 ºC for the remaining primary solvents (CB, o-xy). *n*-doped Si (100) polished wafers on both sides purchased from Neyco were used as substrates. Prior to casting, the silicon substrates were cleaned by consecutive sonication baths in acetone and then in 2-propanol. Afterwards, the substrates were dried with air and placed in an ozone cleaner (Ossila Ltd.) for 15 minutes.

Grazing incidence wide-angle X-ray scattering (GIWAXS) measurements: these experiments were performed at the BL11 NCD-SWEET beamline at ALBA Synchrotron Radiation Facility (Spain). The incident X-ray beam energy was set to 12.4 keV using a channel cut Si (1 1 1) monochromator. The angle of incidence was set between 0.1-0.15° to ensure surface sensitivity. The scattering patterns were recorded using a Rayonix® LX255-HS area detector, which consists of a pixel array of 1920 × 5760 pixels (H × V) with a pixel size of 44 × 44 μm^2. Data are expressed as a function of the scattering vector (q), which was calibrated using Cr_2O_3 as standard sample, obtaining a sample to detector distance between 145.6 and 200.93 mm depending on the beamtime. 2D GIWAXS patterns were corrected as a function of the components of q. Edges of the samples were removed to eliminate edge effects in the GIWAXS experiments. To perform the analysis of the diffraction patterns, the 2D patterns were integrated, corrected with respect to the reference and the 1D profiles were extracted using the Fit2D piece of software. The linecuts were fitted using PseudoVoigt functions together with an exponential decay function as background in Fityk.[1] The crystalline coherence length (CCL) was computed as

$$CCL = \frac{2\pi K}{FWHM},$$

where K is a shape factor (0.9) and FWHM refers to the full width at half maximum of the selected peak centered at q. On the other hand, the paracrystallinity disorder parameter g was calculated as

$$g(\%) = \sqrt{\frac{FWHM}{2\pi q}}$$

Grazing incidence small-angle X-ray scattering (GISAXS) measurements: GISAXS experiments were conducted at the NCD-SWEET beamline of ALBA synchrotron (Spain). A monochromatic X-ray beam with an energy of 12.4 keV was shone on the samples with an incidence angle of 0.12° and 0.15°. The exposure time was 1 s and the sample to detector distance was 2.54 m. The 2D patterns were recorded with a Pilatus3 S 1 M detector, which consists of a pixel array 1043 × 981 (V × H) pixels of 172 × 172 μm^2. Horizontal line q_y cut profiles were done at the Yoneda peak. Edges of the samples were removed to eliminate edge effects in the GISAXS scattering pattern.

Raman and photoluminescence (PL) measurements: Raman and PL spectra were acquired in air with a WITec Alpha 300 RA confocal microscope coupled with an Olympus objective with 10X magnification using a 488 nm (Raman) or 633 nm (PL) laser as excitation source. Raman spectra were background-corrected and fitted with Lorentzian line shapes in Fityk.[1]

Organic photovoltaic device preparation: the organic solar cells were prepared in inverted architecture. Pre-patterned ITO coated glass (25x75 mm, Ossila Ltd.) featuring 24 pixels of 8 mm^2 each were used as substrates and transparent electrode. After their sequential cleaning in a bath sonicator, the electron transport layer made of ZnO (nanoparticles dispersion N-10, obtained from Avantama) was blade coated (ZUA 2300, Zehntner) and annealed at 100 ºC for 10 minutes in air. Substrates were then transferred to a nitrogen-filled glovebox where the PAL deposition took place by blade coating (20 mg mL^{-1}). By purposely decelerating the applicator from a coating speed of 99 mm s^{-1} down to 1 mm s^{-1}, a lateral thickness gradient was formed as a high-throughput approach to study the PAL thickness influence on the device performance. After PAL deposition, no further annealing treatments were performed. Following, the hole transporting layer (MoO_x) and the silver top contacts were thermally evaporated.

J-V curve characterization under illumination: The current-voltage characteristics (*J-V*) of the OPV devices were extracted using a Keithley 2400 source meter and an Arduino-based multiplexer and switcher. All the electronic components were automatically controlled with a LabView software tool that allows the fast measurement of 24 devices in less than 6 minutes. As illumination source, a solar simulator (XES-100S, SAN-EI Electric) providing a calibrated and certified AM1.5G (Air Mass 1.5 Global) spectrum with an irradiance of 100 $mW \cdot cm^{-2}$ was employed. The solar simulator was calibrated with a certified silicon solar cell (Oriel, Newport).

External quantum efficiency (EQE) measurements: EQE spectra were measured with a homemade setup that uses a Supercontinuum light source (LLTF contrast, Fianium) coupled to a monochromator filter and normalized by the light power as measured by a silicon diode. EQEs were recorded from 400 nm to 900 nm excitation wavelength by focusing the 50 μm diameter laser spot. The setup was controlled with LabView-based software.

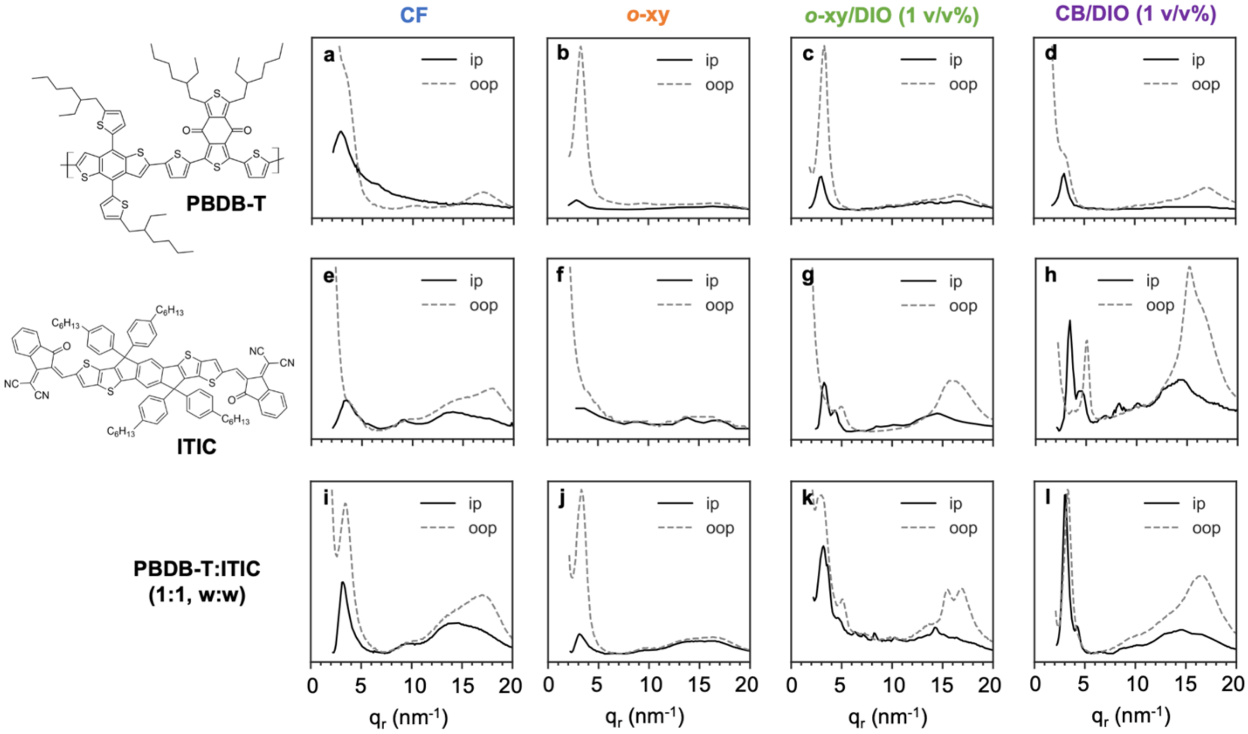

Figure S1. GIWAXS linecuts of PBDB-T (a-d), ITIC (e-h) and their 1:1, w:w blend (i-l) as processed from four different co-solvent formulations: chloroform (CF, first column), o-xylene (o-xy, second column), o-xylene:DIO (99:1, v:v, third column) and chlorobenzene:DIO (99:1, v:v, fourth column). The integration directions are defined as *ip* (in-plane, solid black curves) and *oop* (out-of-plane, dashed grey curves).

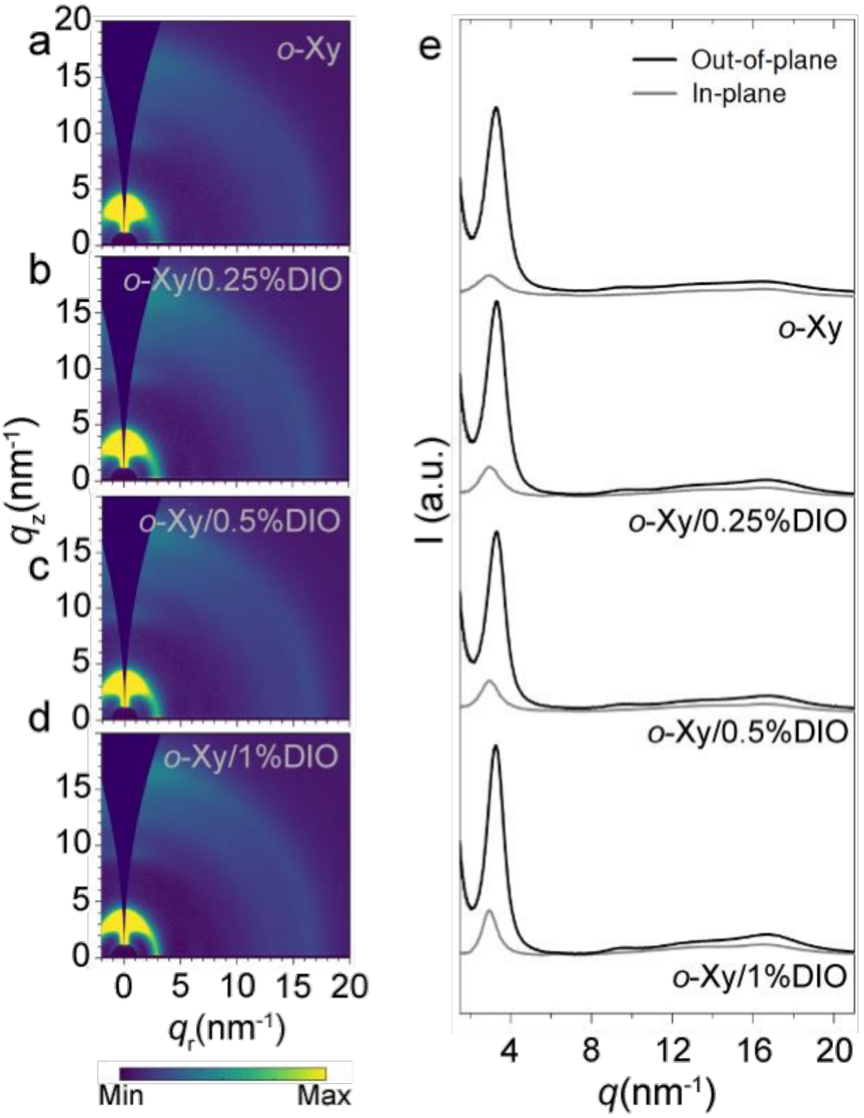

Figure S2. 2D GIWAXS patterns of PBDB-T spun cast from (a) neat o-xylene (o-xy); and different o-xy/1,8-diiodooctane (DIO) mixtures, namely (b) o-xy and 0.25 v/v% DIO; (c) o-xy and 0.5 v/v% DIO; and (d) o-xy and 1.00 v/v% DIO. (e) The corresponding integrated out-of-plane and in-plane linecuts.

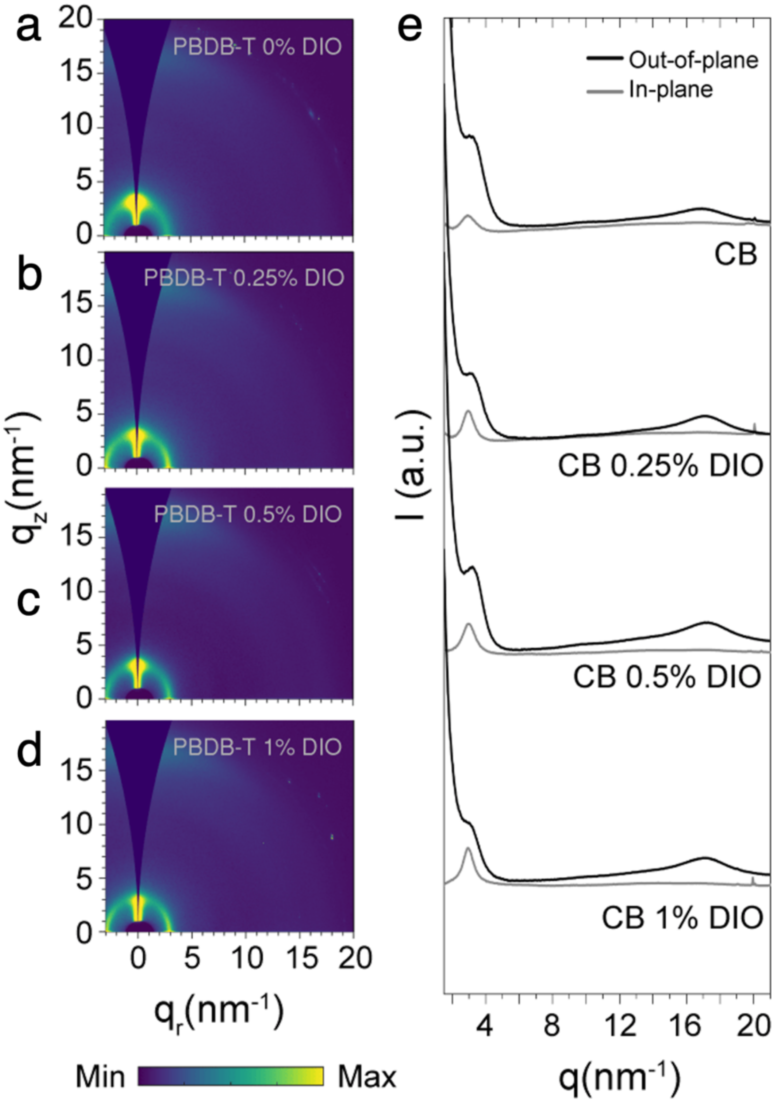

Figure S3. 2D GIWAXS patterns of PBDB-T spun cast from (a) neat chlorobenzene (CB); and different CB/1,8-diiodooctane (DIO) mixtures, namely (b) CB and 0.25 v/v% DIO; (c) CB and 0.5 v/v% DIO; and (d) CB and 1.00 v/v% DIO. (e) The corresponding integrated out-of-plane and in-plane linecuts.

Table S1. Hansen solubility parameters of PBDB-T and the co-solvents used in this work. R_a corresponds to the distance between PBDB-T and each of the solvents in the Hansen space calculated according to the formula: $R_a^2 = 4(\delta D_{PBDB-T} - \delta D_{solvent})^2 + (\delta P_{PBDB-T} - \delta P_{solvent})^2 + (\delta H_{PBDB-T} - \delta H_{solvent})^2$. B.P. refers to 'boiling point'.

Material / Solvent	**δD (MPa$^{1/2}$)**	**δP (MPa$^{1/2}$)**	**δH (MPa$^{1/2}$)**	**R_a (MPa$^{1/2}$)**	**B.P. (°C)**	**Ref.**
PBDB-T	18.9	2.5	7	N/A	N/A	[2]
CF	17.8	3.1	5.7	2.6	61	[3]
o-xy	17.8	1	3.1	4.7	144	[3]
CB	19	4.3	2	5.3	132	[3]
DIO	18.1	3.8	3.3	4.2	332	[4]

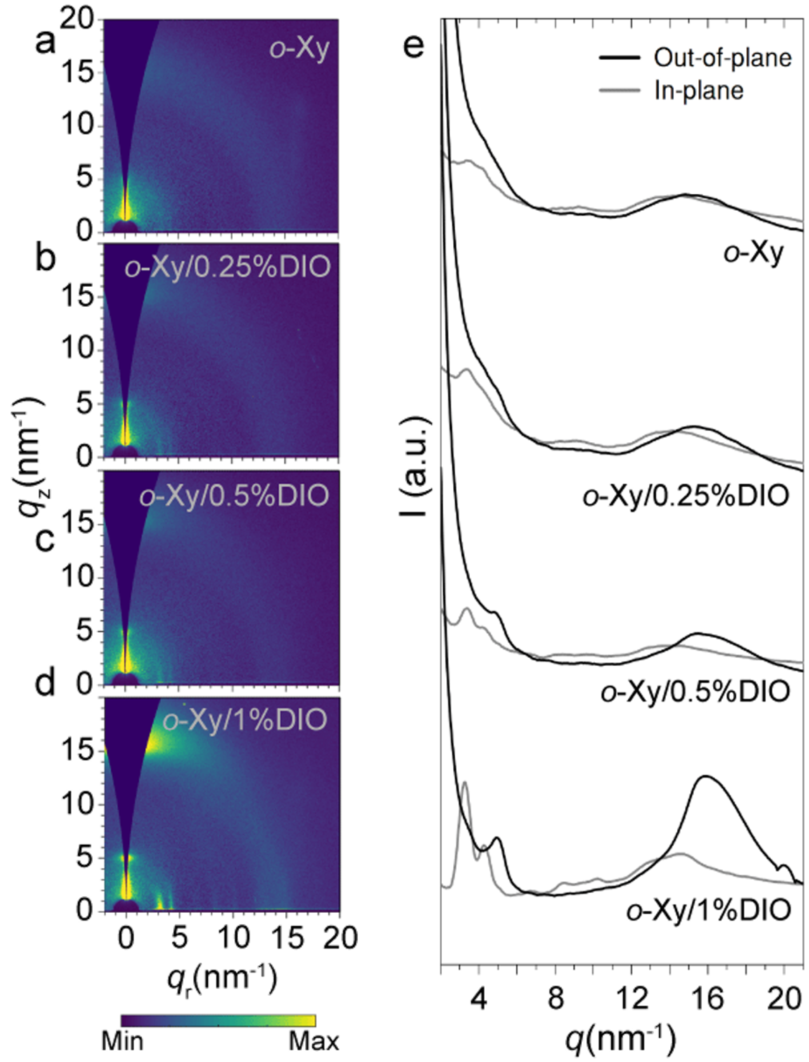

Figure S4. 2D GIWAXS patterns of ITIC spun cast from (a) neat o-xylene (o-xy); and different o-xy/1,8-diiodooctane (DIO) mixtures, namely (b) o-xy and 0.25 v/v% DIO; (c) o-xy and 0.5 v/v% DIO; and (d) o-xy and 1.00 v/v% DIO. (e) The corresponding integrated out-of-plane and in-plane linecuts.

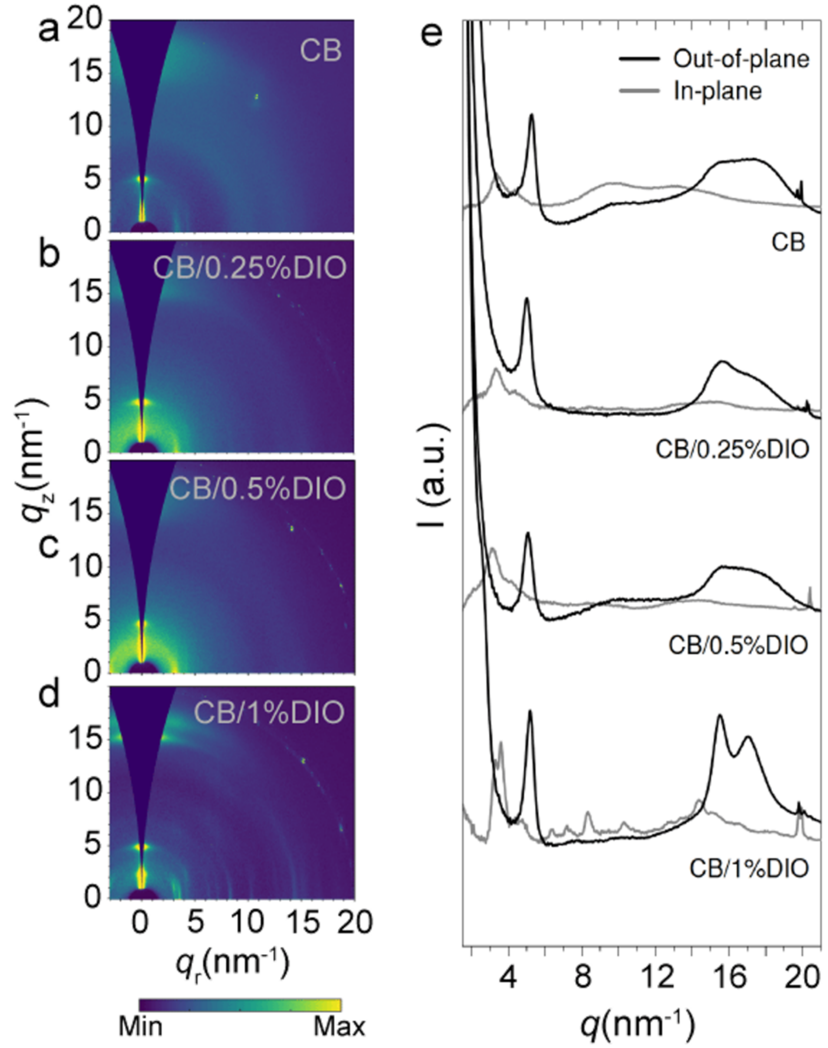

Figure S5. 2D GIWAXS patterns of ITIC spun cast from (a) neat chlorobenzene (CB); and different CB/1,8-diiodooctane (DIO) mixtures, namely (b) CB and 0.25 v/v% DIO; (c) CB and 0.5 v/v% DIO; and (d) CB and 1.00 v/v% DIO. (e) The corresponding integrated out-of-plane and in-plane linecuts.

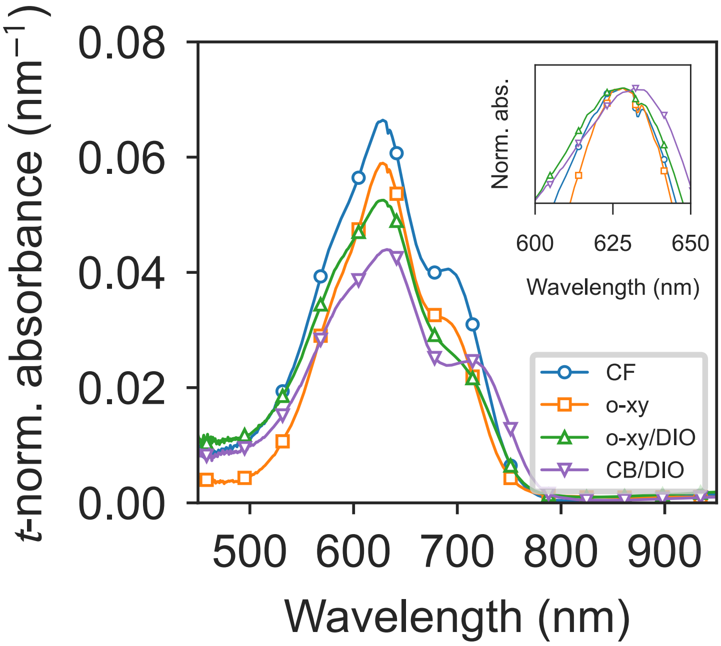

Figure S6. Absorbance normalized per nanometre of thickness of PBDB-T:ITIC 1:1, w:w, blend films spin-coated from chloroform (CF), o-xylene (o-xy), o-xylene:1,8-diiodooctane (o-xy:DIO, 99:1, v:v); and chlorobenzene:DIO (CB:DIO, 99:1, v:v).

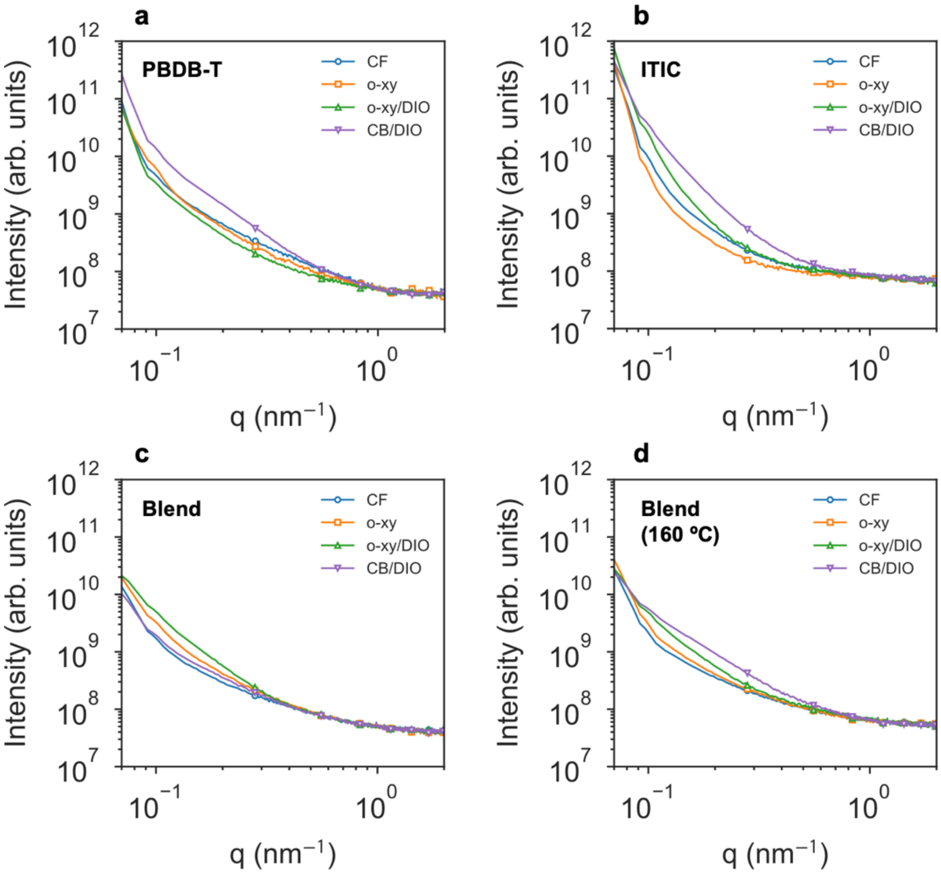

Figure S7. GISAXS horizontal cuts of (a) PBDB-T, (b) ITIC, and their (c) as-cast and (d) annealed blends (1:1, w:w) spin-coated from chloroform (CF), o-xylene (o-xy), o-xylene:1,8-diiodooctane (o-xy:DIO, 99:1, v:v); and chlorobenzene:DIO (CB:DIO, 99:1, v:v).

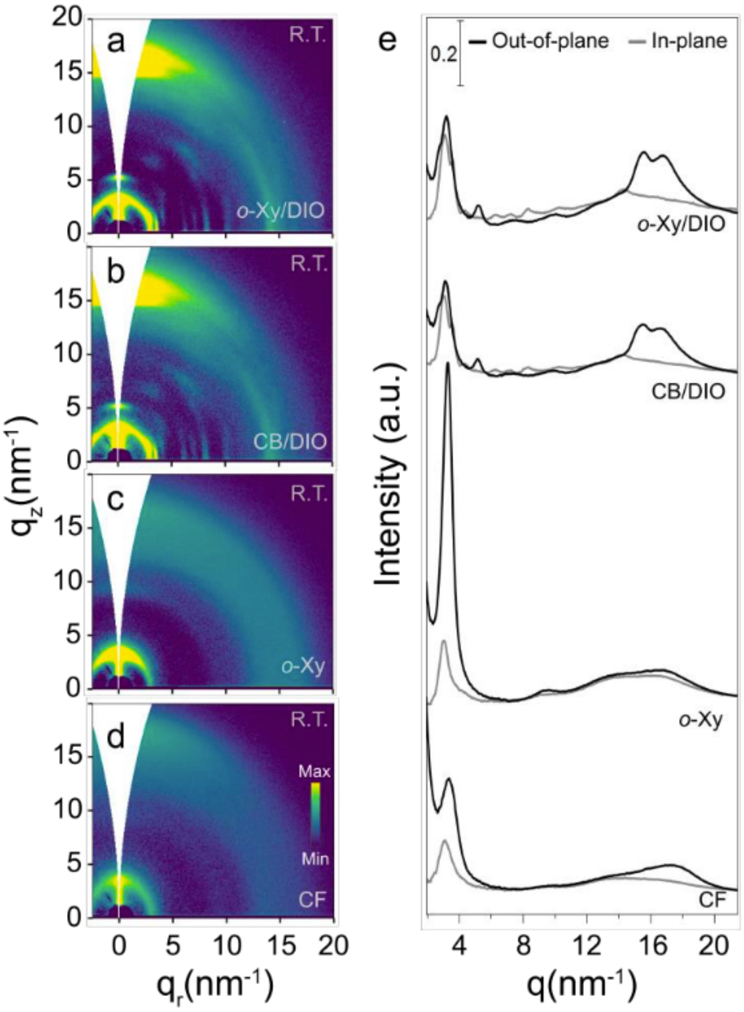

Figure S8. 2D GIWAXS patterns of PBDB-T:ITIC 1:1, w:w, blends blade coated from (a) o-xylene:1,8-diiodooctane (o-xy:DIO, 99:1, v:v), (b) chlorobenzene:DIO (CB:DIO, 99:1, v:v), (c) o-xylene (o-xy), and (d) chloroform (CF). (e) The corresponding out-of-plane and in-plane integrated linecuts.

Table S2. Benchmark reported PCEs of organic solar cells including the PBDB-T:ITIC blend as photoactive layer. Abbreviations correspond to: CB = chlorobenzene; DIO = 1,8-diiodooctane; CF = chloroform; o-xy = ortho-xylene; SC = spin-coating; BC = blade coating.

PCE (%)	**Primary solvent**	**Co-solvent**	**Device structure**	**Coating method**	**Reference**
11.84	CB	1,3,5-trichlorobenzene	**Inverted** (ZnO/MoO_3/Ag)	**SC**	5
11.21	CB	0.5 vol% DIO	**Inverted** (ZnO/MoO_3/Al)	**SC**	6
11	CB	0.5 vol% DIO	**Conventional** (PEDOT:PSS/PFN-Br/Ag)	**SC**	7
10.9	CB	0.5 vol% DIO	**Inverted** (ZnO+SAM/MoO_3/Ag)	**SC**	8
10.75	CB	0.5 vol% DIO	**Inverted** (ZnO/MoO_3/Ag)	**SC**	9
10.1	CB	0.5 vol% DIO	**Conventional** (PEDOT:PSS/PDINO/Al)	**SC**	10
10.2	CB	1,8-octanedithiol	**Conventional** (PEDOT:PSS/ZrAcac/Al)	**BC**	11
10.03	CB	0.25 vol% DIO	**Inverted** (ZnO/MoO_3/Al)	**BC**	12
9.57	CB	0.5 vol% DIO	**Inverted** (ZnO/MoO_3/Ag)	**BC**	13
9.76	**CF**	**None**	**Inverted** (ZnO/MoO_3/Ag)	**BC**	**This work**
8.65	**o-xy**	**None**	**Inverted** (ZnO/MoO_3/Ag)	**BC**	**This work**

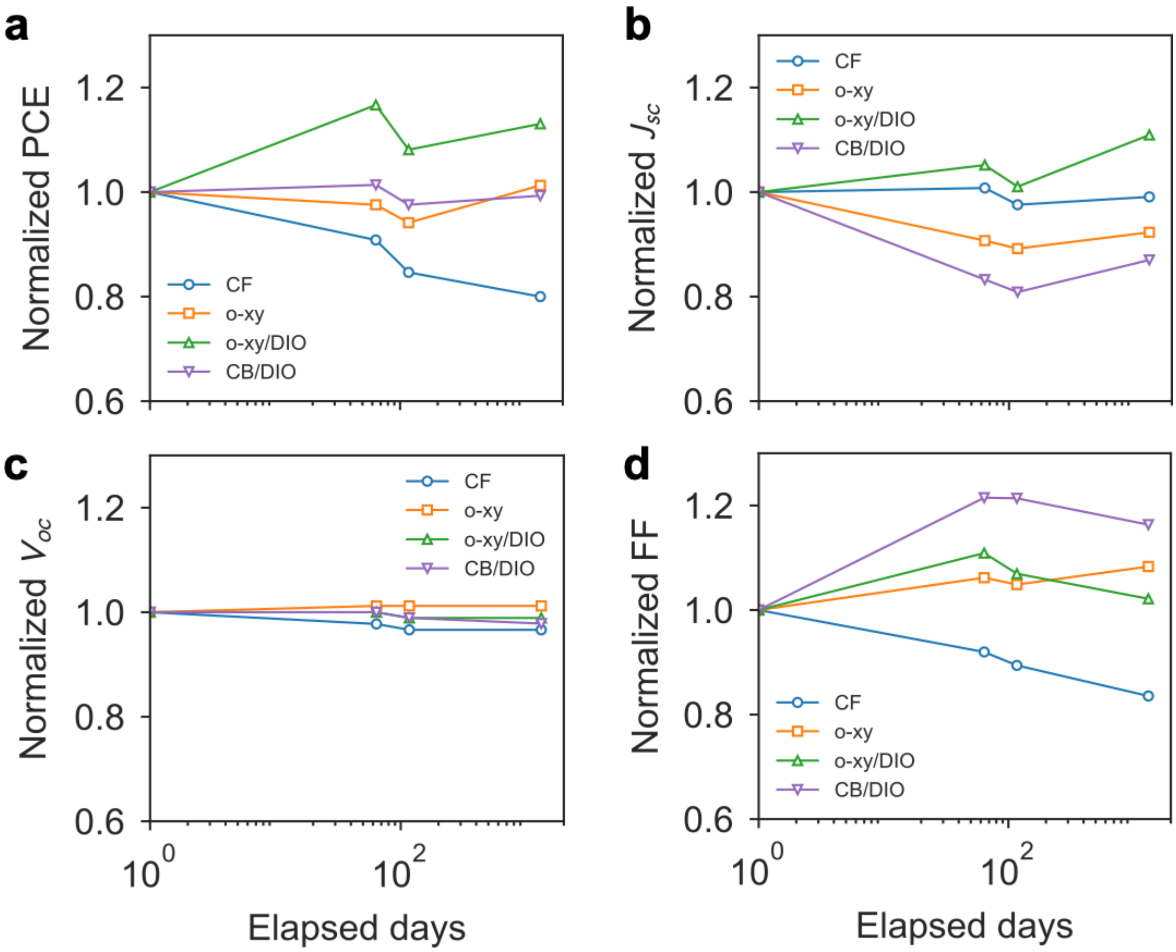

Figure S9. Photovoltaic figures of merit of selected devices subject to a shelf stability study for a period of 1322 days: (a) PCE, (b) J_{sc}, (c) V_{oc} and (d) FF. Data are normalized to the value acquired at the start of the study. To adequate the logarithmic scale, the starting measurement was set on day 1 (rather than day 0).

Supplementary References

1 M. Wojdyr, *Journal of Applied Crystallography*, 2010, **43**, 1126–1128.

2 Y. Liu, Q. Fan, H. Liu, I. Jalan, Y. Jin, J. V. Stam, E. Moons, E. Wang, X. Lu, O. Inganäs and F. Zhang, *J. Phys. Chem. Lett.*, 2022, **13**, 11696–11702.

3 C. M. Hansen, *Hansen Solubility Parameters: A User's Handbook, Second Edition*, CRC Press, 0 edn., 2007.

4 G. Tostado-Blázquez, KAUST Research Repository, 2021.

5 J. Fu, P. W. K. Fong, H. Liu, C.-S. Huang, X. Lu, S. Lu, M. Abdelsamie, T. Kodalle, C. M. Sutter-Fella, Y. Yang and G. Li, *Nat Commun*, 2023, **14**, 1760.

6 W. Zhao, D. Qian, S. Zhang, S. Li, O. Inganäs, F. Gao and J. Hou, *Advanced Materials*, 2016, **28**, 4734–4739.

7 R. C. Kilbride, E. L. K. Spooner, E. J. Cassella, M. E. O'Kane, K. Doudin, D. G. Lidzey, R. Jones and A. J. Parnell, *ACS Appl. Energy Mater.*, 2024, **7**, 8401–8411.

8 S. Zhang, L. Zhan, S. Li, C.-Z. Li and H. Chen, *Organic Electronics*, 2018, **63**, 143–148.

9 L.-M. Wang, Q. Li, S. Liu, Z. Cao, Y.-P. Cai, X. Jiao, H. Lai, W. Xie, X. Zhan and T. Zhu, *ACS Appl. Mater. Interfaces*, 2020, **12**, 24165–24173.

10 B. Lee, M. Jeong, J. Lee, J. Oh, Y. Cho, S. Jung, S. M. Lee, S. Chen and C. Yang, *Solar RRL*, 2019, **3**, 1900033.

11 L. Zhang, H. Zhao, J. Yuan, B. Lin, Z. Xing, X. Meng, L. Ke, X. Hu, W. Ma and Y. Yuan, *Organic Electronics*, 2020, **83**, 105771.

12 L. Zhang, B. Lin, B. Hu, X. Xu and W. Ma, *Advanced Materials*, 2018, **30**, 1800343.

13 S. H. Park, S. Park, S. Lee, J. Kim, H. Ahn, B. J. Kim, B. Chae and H. J. Son, *Nano Energy*, 2020, **77**, 105147.